Supporting Information

Framework mutations incorporated into library to improve expression

We determined that solubilizing mutations described in Olson *et al*., 2008 universally enhance expression of our library, which we term e10Fn3.[1] These mutations include A12E and L19Q, which are polar substitutions at two adjacent surface exposed hydrophobic residues (Figure S1a, numbering reflects conventional 10FnIII positions where reference 1 employed numbering based on the start Met in our Δ1-7 truncated library). The T14S mutation was selected in connection with mutation of position 12 during the first round of screening, and may also contribute to solubility (see reference 1). The L18I mutation may improve stability due to improved core packing interactions, or as a result of the improved propensity to form β-sheets among β-branched amino acids.[2, 3] Using the GFP folding reporter assay, these four mutations (A12E, T14S, L18I, and L29Q, denoted C25) were tested for expression enhancement in four variants not related in sequence with varying levels of wild type expression yield (Figure S2b). All four gained between 16% and 80% of initial expression values (which are represented relative to wild type 10FnIII without engineered loop regions). An additional hydrophobic to polar surface mutation, V11K, matching the identity of the third FnIII domain of tenascin, was previously found to improve expression of FnIkB-10C17. We tested the ability for this mutation to improve expression of two different clones, Fn38 and Fn-N17, and both were enhanced (Figure S1a,b). A large enhancement in expression is also seen in the *in vitro* expression system employed in our selections. Remarkably we found a 2-4-fold improvement in protein yield in this format, even greater improvement than the bacterial system in which the mutations were evolved. An interesting result of our solubility evolution is that the FnIkB-10C17 binding efficiency is enhanced by the C25 mutations, which we argue is a consequence of increased stability and confirms that the mutations do not alter the structure.[1] We investigated the affect of these mutations on the binding of the SARS nucleoprotein-binding Fn-N10, Fn-N17, and Fn-N22 to determine if they affect function. While binding did not improve, it was only marginally less efficient (Figure S1d) indicating the loop context is not largely perturbed by these mutations.

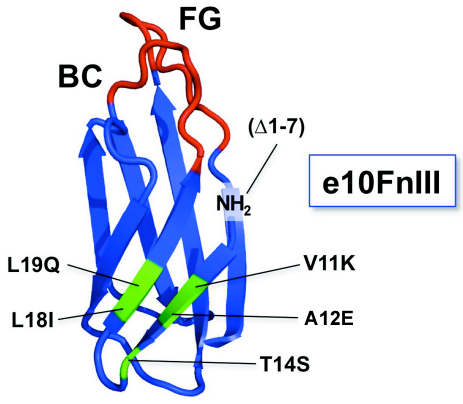

Figure S1a. Illustration of 10Fn3 domain with solubilizing mutations.

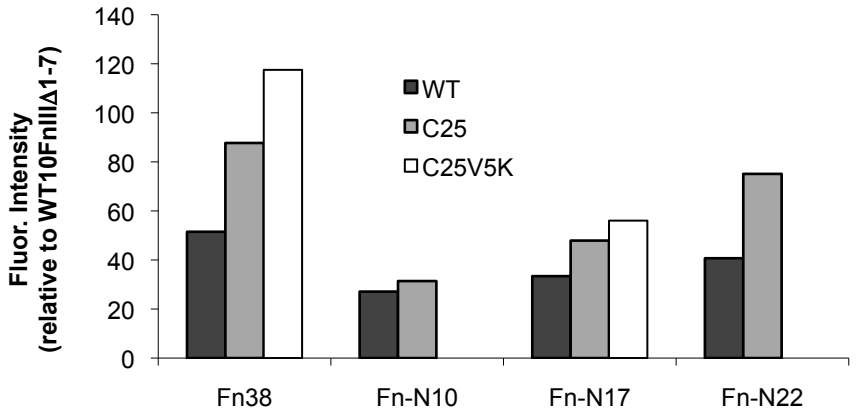

Figure S1b. Fluorescence assay to quantify enhancement in protein expression as described in Waldo *et al*. 1999[4] and Olson *et al.* 2008.[1] The C25 mutations were generated with the non-selected Fn38[5] and SARS N binders Fn-N10, -N17, and –N22.[6] After Fn-GFP fusions were expressed in BL21(DE3), normalized cells were resuspended in cold PBS and whole cell fluorescence intensities were measured. We tested an additional rational mutation at a highly solvent-exposed position (V5K) and found this mutation to further enhance expression of Fn38 and Fn-N17, as well as Fn-10C17 (data not shown). V5H or V5N have little to no effect on protein expression.

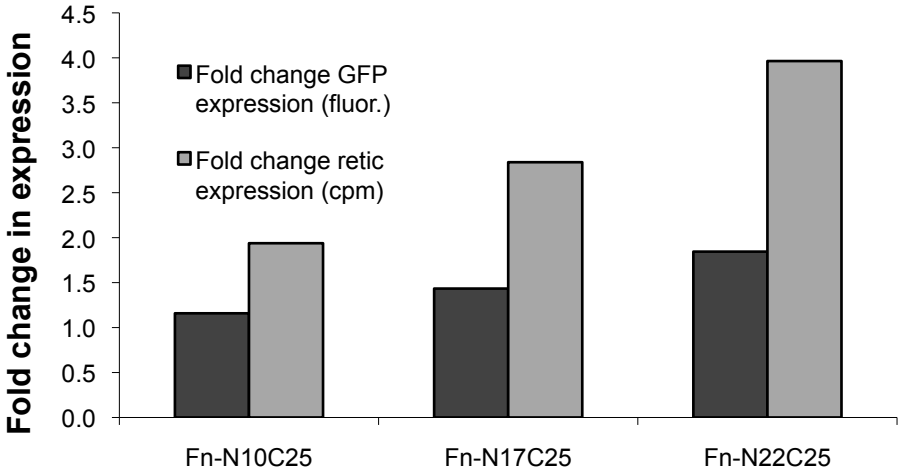

Figure S1c. *In vitro* expression yield is also increased by the C25 mutations. Fn3 RNA was translated with rabbit reticulocyte lysate and ^{35}S-Met labeled proteins were purified by M2 anti-Flag agarose followed by scintillation counting.

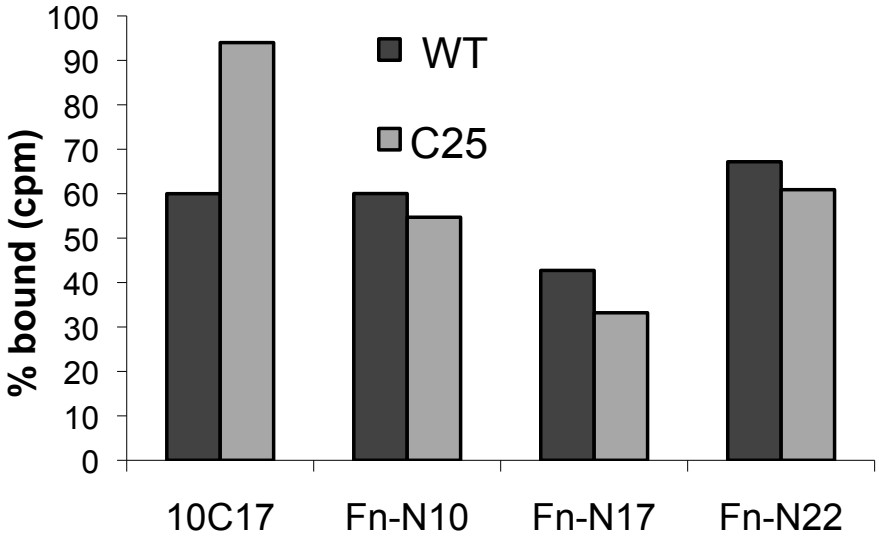

Figure S1d Pull-down efficiency of the phospho-IkBa binder 10C17 and three SARS N binders with or without C25 mutations. In vitro translated ^{5}S-Met labeled proteins were purified by M2 anti-Flag agarose, and bound to beads immobilized with target and washed 5 times with TBS, 0.05% tween. Flow through, washes and beads were scintillation counted.

Background binding

We initially tested background binding against streptavidin-coupled or carboxylic acid-coated M-270 Dynabeads using ^{35}S-methionine-labeled random peptide mRNA fusions and found significant background binding (~1.5% and 1.2%, respectively; Figure S1). Fusions were prepared as described previously (see below), bound to beads in binding buffer (50 mM HEPES-KOH pH 7.5, 150 mM NaCl, 0.05% (v/v) Tween-20, 1 mM EDTA, 1 mg/mL BSA, and 10 mg/µL yeast tRNA), and washed in batch with a magnetic bead collector. All fractions were subsequently scintillation counted (Beckman Coulter, Brea, CA). Background binding to both streptavidin and carboxylic acid beads could be reduced to ~0.02% by incubation with 1 M NaCl, potentially indicating inefficiency in carboxylate blocking or NHS hydrolysis, which could result in strong ionic interaction between peptides and beads. We next tested epoxy M-270 beads loaded with neutravidin (immobilized per manufacturer's specifications) and found low background (<0.02%) in binding buffer.

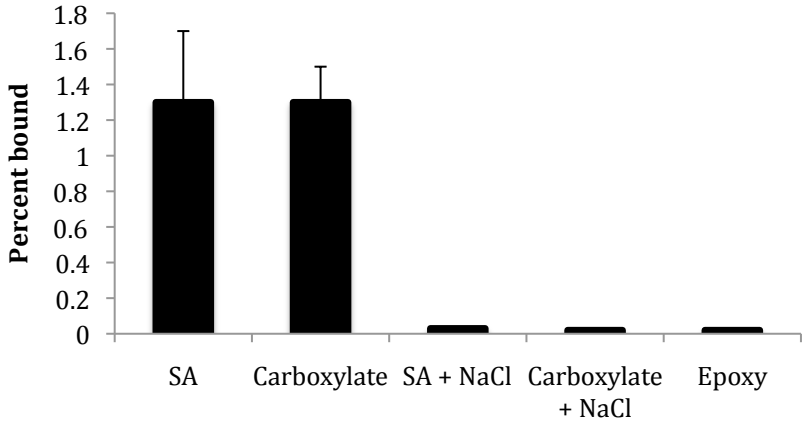

Figure S2. Background binding test with magnetic beads. ^{35}S-Methionine labeled fusions (MX10K)[7] fusions were prepared as described and bound to 10^6 beads in binding buffer (See text for details). After 5 washes, all fractions and beads were collected for scintillation counting.

Iodoacetamide modification inhibits pool 3A binding to IL-6

IL-6 contains two solvent exposed disulfide bonds, one of which is important for function.[8] We therefore implemented an iodoacetamide blocking step in order to eliminate free thiols enabling the selection to be performed in oxidizing conditions, thereby preserving the native state of IL-6. Iodoacetamide blocking inhibited binding of pool 3A to IL-6, enabling the selection of non-cysteine-containing clones in selection "B".

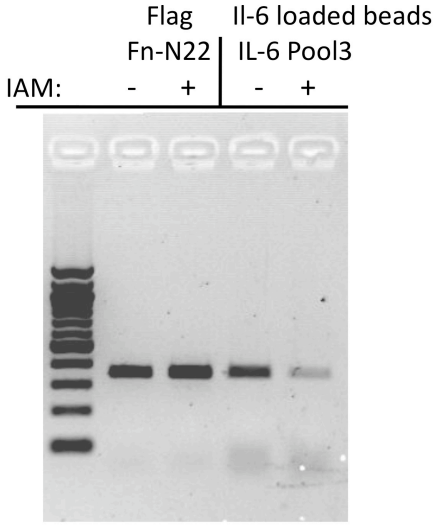

Figure S3. Mock selection with iodoacetamide (IAM) modification. After elution from M2 agarose beads, an equivalent fraction of each sample was amplified by PCR. Fn-N22, which does not contain cysteines, was used to demonstrate that there is no loss from the procedure, while pool 3A was used to determine if cysteine modification reduces binding to IL-6.

Detailed Methods

Bead preparation. Based on their low intrinsic background binding characteristics, we chose neutravidin-coupled epoxy M270 Dynabeads (Invitrogen, Carlsbad, CA) for our CFMS selection, prepared as per manufacturer's specifications. Briefly, we incubated 1 mg/ml neutravidin (Pierce/Thermo Fisher Scientific, Rockford, IL) in 100 mM sodium phosphate buffer with 1 M ammonium sulfate with 10^9 beads for 48 hours at room temperature, followed by blocking with TBS. Recombinant IL-6 (Cell Signaling Technologies, Danvers, MA) was conjugated with sulfo-NHS-LC-biotin (Pierce) per manufacturer's recommendations: 50 μM IL-6 and 250 μM sulfo-NHS-LC-biotin in PBS, incubated for 30 minutes at room temperature. We immobilized 5 μg of IL-6 onto $5x10^6$ neutravidin-conjugated beads for round 1; for subsequent rounds, 1 μg of IL-6 was immobilized onto $1x10^6$ neutravidin-conjugated beads followed by extensive washing and blocking with biotin.

Continuous flow magnetic separation (CFMS). Three 0.25"×0.25"×0.5" NdFeB magnets (B448, K & J Magnetics, Inc., Jamison, PA) were affixed to ~10 cm of PFA tubing (0.0625" outer diameter, 0.04" inner diameter). The PFA tubing was attached to a syringe pump (SP1000, Next Advance, Averill Park, NY) which was used to withdraw the bead slurry and washing buffer at a flow rate of 30 mL/h. We estimated the performance of the system by simulating the depletion of beads from the suspension to the surface of the tube using COMSOL Multiphysics 3.5 (Burlington, MA). In our simulation, we assumed the beads were not self-interacting. We modeled the capture of beads at the surface of the tube using a modified convection-diffusion equation that accounted for the magnetic force on the beads.

We numerically solved the Navier-Stokes equation for fluid flow within the tube, and Maxwell's equations for the magnetic field due to the permanent magnets. Using the solutions to these equations for our system, we defined the bead convection velocity $\vec{v}$ as

$$\vec{v} = \frac{m\nabla B}{6\pi\eta a} + \vec{u}$$

where m is the saturation magnetization of the beads (2.299×10^{-13} A·m^2 as provided by the manufacturer), B is the magnitude of the magnetic field as solved numerically, η is the viscosity of the fluid, a is the bead

radius, and $\vec{u}$ is the fluid velocity in the tube as solved numerically. We then solved for the concentration of beads within the tube, assuming a diffusion coefficient of 10^{-7} m^2/s. The diffusion coefficient was chosen to be much larger than that given by the Stokes-Einstein equation ($\sim 10^{-13}$ m^2/s) in order to facilitate the simulation. The input concentration of the beads was specified at 2×10^6 beads/mL. To account for capture of beads at the surface, we allowed for convective flux of the beads through the boundary of the tube closest to the magnets. Because the convective forces dominate over diffusive forces, bead flux upwards from this surface would be negligible and therefore this boundary condition accurately models the system while simplifying the analysis. The simulation shows that the bead concentration is reduced by over four orders of magnitude as a result of magnetic capture.

In addition to attracting the beads towards the surface of the tube, the magnetic force must retain the beads against the fluidic drag force. The drag force on a bead is given by Stokes' drag, with stationary beads experiencing maximum drag force. The results of our simulation showed that there are four regions in the proximity of the tube wall where the magnetic force in the horizontal direction exceeds the maximum potential horizontal fluidic drag force. These regions are located close to the edges of the magnets and extend approximately 30 μm into the fluid from the wall of the tube.

We performed bead consolidation and washing experiments in triplicate, and used FACS analysis (FacsARIA, BD Biosciences, Franklin Lakes, NJ) to determine the efficiency of bead recovery. 10^6 neutravidin-conjugated M270 beads bound with biotin-phycoerythrin were suspended in 500 μl TBS plus 0.05% Tween-20 and withdrawn into the tubing at 30 mL/h, then washed five times with 500 μl buffer for ~5 minutes, after which the flow was stopped. Approximately 2 cm of tubing (~15 μl) corresponding to the region attached to the magnets were excised and placed into 485 μl of fresh buffer. The microcentrifuge tube initially containing the bead suspension was washed with 500 μl of fresh buffer for analysis. Equivalent samples from each of the three sources were analyzed via flow cytometry; in two of the three, no beads were detected in the flowthrough, with an overall average of 0.01% bead loss. The microcentrifuge tube containing the bead suspension before washing was found to contain ~8.2% of the total beads, indicating that a wash step would enhance bound library recovery. However, this fraction is small compared to the ~10-fold coverage contained in our round one library (pool 0).

Library construction. The library was assembled as described previously,[5,6] except with modification of the following oligos to incorporate C25 mutations and limit randomization of BC loop position 7 (see online supporting information): FnOligo3 (5' - ACC AGC ATC CAG ATC AGC TGG NNS NNS NNS NNS NNS NNS VTT CGC TAC TAC CGC ATC ACC TAC G), FnOligo2C25K (5' - CA ATT ACA ATG CTC GAG GTC AAG GAA GCA TCA CCA ACC AGC ATC CAG ATC AGC TGG), and FnOligo1C25K (5'- TTC TAA TAC GAC TCA CTA TAG GGA CAA TTA CTA TTT ACA ATT ACA ATG CTC GAG GTC AAG G).

mRNA-Fn3 fusion synthesis. mRNA-peptide fusions were prepared as described previously.[6,9] For round one, 1×10^{12} unique clones were amplified by PCR (KOD polymerase, EMD Biosciences, San Diego, CA) with FnOligo9 (5'- GGA GCC GCT ACC CTT ATC GTC GTC ATC CTT GTA ATC GGA TCC GGT GCG GTA GTT GAT GGA GAT CG) and FnOligo1C25K (above). The PCR amplified library was transcribed *in vitro* in a 1 ml reaction volume using T7 RNA polymerase and purified by phenol/chloroform extraction, ethanol precipitation and gel filtration (illustra NAP-5, GE Healthcare, Waukesha, WI). 10 nmol of RNA was ligated to 12 nmol of pF30P linker (5'- phospho-$(A)_{20}$-$(spacer9)_3$-ACC-puromycin), mediated by 11 nmol of a splint oligonucleotide (5'- TTT TTT TTT TTT GGA GCC GCT ACC) with T4 DNA ligase (New England Biolabs, Ipswich, MA) in 1 ml reaction volume. The ligated library was purified by denaturing urea PAGE and extracted by electro-elution. One thousand pmol of mRNA was translated with rabbit reticulocyte lysate (Ambion, Austin, TX) in a 2.5 ml reaction volume. Enhanced fusion formation was induced by addition of KCl (500 mM final) and $MgCl_2$ (60 mM final). Pool 0 fusions were purified by binding against 50 mg oligo-dT cellulose (Invitrogen) in 25 ml of 100 mM Tris (pH 8), 1 M NaCl, and 0.2% Triton X-100 at 4 °C. After washing, fusions were eluted at room temperature with three aliquots of 5 mM Tris, pH 8, totaling 2.5 ml. Fusions were buffer-exchanged into reverse transcription buffer with a NAP-25 gel filtration column (GE Healthcare) and reverse-transcribed with 7,000 U of Superscript II reverse transcriptase (Invitrogen). In subsequent rounds of selection, reactions were scaled down as follows: 400 μl PCR, 200 μl transcription reactions, 200 μl splint ligation, 100 μl translation volume (40 pmol), fusion purification with 2 mg oligo-dT cellulose eluted in 80 μl, spin desalting (Princeton Separations, Adelphia, NJ), and 100 μl reverse transcription (200U SSII). All selection rounds following round 1 included a pre-selection by purifying with M2 anti-FLAG agarose beads (Sigma-Aldrich, St. Louis, MO) in TBS plus 0.05% Tween-20, eluted with buffer plus 3XFLAG peptide (150 μg/ml).

Selection A. After reverse-transcription, pool 0 fusions were diluted to 5 ml in conditions replicating binding buffer (TBS plus 0.05% Tween-20, 1 mg/ml BSA). The sample was incubated with 5×10^6 beads loaded with IL-6 for one hour at room temperature followed by CFMS as described above. Round 2A was scaled down as described, with binding performed against 1×10^6 beads; round 2A cDNA was amplified after 27 cycles of PCR. Round 3A cDNA was amplified in 24 cycles of PCR, indicating that pool 2A binds above background. A mock round of selection was then performed with and without target to test binding of pool 3A. Only 16 cycles of PCR were required to amplify pool 3A cDNA in the presence of target, while pool 3A bound to beads without target required 28 cycles of PCR for amplification, indicating that binding is specific. Pool 3A was cloned into pAO5,[1] and sequencing of ten clones indicated that the pool was highly convergent (Figure 2). Seven of ten clones were identical (eFn-3A02) and the remaining three were unique (eFn-3A01, eFn-3A03 and eFn-3A06). All but one contained cysteines, which may mediate binding to IL-6 but may also be undesirable for a number of reasons. For example, two or more free cysteines can mediate oligomerization (observed upon expression of eFn-3A02). Also, cysteines may cause non-specific

disulfide bonding to non-target proteins. Finally, the absence of cysteines in the 10Fn3 scaffold represents a useful feature, providing an orthogonal "handle" for conjugation of molecular probes, polymers, or surfaces.[10]

Selection B. In order to provide a selective advantage for clones that do not contain cysteines, we investigated methods to remove cysteine-containing clones or chemically modify cysteine residues. Simply conducting the selection in a reducing environment was not desirable due to the requirement for disulfide bonds for IL-6 function. We first tested depletion of cysteine-containing clones using iodoacetamide functionalized resin or activated thiol resin. However, neither of these methods were compatible with our mRNA display selection due to loss of sample (data not shown). We next tried chemically modifying cysteine residues with iodoacetamide (Sigma), which modifies cysteine side chains to a thioether and thereby prevents disulfide bond formation. After oligo-dT cellulose purification, we treated fusions with 1 mM iodoacetamide in TBS for 30 minutes at room temperature, then terminated the reaction by addition of dithiothreitol (DTT), followed by desalting through a spin column (Princeton Separations). To determine the efficacy of this procedure, we tested a mock round of selection using Fn-3A02 with or without iodoacetamide modification. PCR was used to qualitatively demonstrate that modification inhibits binding (Figure S3). We also tested the yield of fusion production by measuring binding of cysteine-free clones to M2 agarose beads with or without modification (Figure S3).

We restarted the selection with pool 1, including the iodoacetamide modification. After three more rounds, we noticed a drop in PCR cycles required for amplification (24 cycles), demonstrating target binding by pool 3B. We sequenced Pool 3B and 4B and found pool 4B to be highly convergent. 16 of 19 clones were identical (eFn-4B02), while the other three represented a second common sequence (eFn-4B01) (Figure 2A). Although pool 3B was more diverse, a clone identical to eFn-4B02 was found once among eight sequenced clones.

Binding signal-to-noise ratio. We determined that binding experiments using the ^{35}S-methionine radionuclide label were not sensitive enough to detect background binding for CFMS experiments. In order to determine the ratio between target and background binding for both CFMS and the traditional batch method, we performed a mock round of selection and quantified relative yield by qPCR (Figure 2B). Pool 4B binding was compared to a diverse control pool composed of full-length fusions that had not been enriched for binding function. Equivalent fusion samples from both the functional and the nonfunctional pools were either bound to 10^6 magnetic beads and separated as before or incubated with 10 µl of neutravidin agarose beads and washed five times. Fusion cDNA was eluted by incubation at 95°C for 10 minutes and serial dilutions were made for qPCR analysis. Six points spanning two orders of magnitude were used to generate a standard curve for pool 4B and the control pool threshold cycles were fit to the standard curve to determine fold recovery.

IL-6 pulldown. In order to demonstrate specific binding to IL-6 we tested pull-down of IL-6 in solution by immobilized e10Fn3s (Figure 2C). We expressed eFn-3A02, eFn-4B01, eFn-4B02, and a control e10Fn3 variant in 5 mL bacterial expression cultures, which were induced for 3 hours with 1 mM isopropyl-β-D-thiogalactopyranoside (IPTG), lysed with B-PER (Pierce) and cleared by centrifugation, after which we immobilized the e10Fn3 variants on 10 μl nickel-NTA agarose. We then incubated these with 1 μg of IL-6 in selection buffer (including 500-fold excess of BSA) for one hour and washed three times in batch. Co-precipitated protein was eluted with SDS-PAGE loading buffer, run on a 15% acrylamide gel, and then transferred to nitrocellulose for western analysis. The blot was probed with rabbit anti-hIL-6 (Abcam, Cambridge, UK) followed by horseradish peroxidase (HRP)-tagged anti-rabbit IgG, and then exposed with enhanced chemiluminescence (ECL) reagents and film.

Binding affinity. We performed surface plasmon resonance (Biacore T100, GE Healthcare) to determine the binding kinetics of eFn4B02 against IL-6 (Figure 2D). eFn4B02 was cloned into pAO9,[1] and expressed and purified as described previously (two-step affinity column purification with nickel-NTA agarose followed by amylose resin (NEB) for MBP-mediated purification). Biotinylated recombinant IL-6 was immobilized onto a streptavidin chip using Biacore's 'immobilization wizard' for biotinylated targets. We set up a kinetics run using concentrations between 10 and 1000 nM, per the manufacturer's recommendation. Binding and dissociation were determined using the Biacore evaluation software. We measured an on-rate of 4.2×10^{4} M^{-1} s^{-1} and an off-rate of 8.8×10^{-4} s^{-1}, resulting in K_D = 21 nM.

Inhibition assay. In order to determine if IL-6 binders were biologically active, we tested inhibition of IL-6-mediated signaling. STAT3 is a transcriptional activator that is phosphorylated downstream after gp130 activation, and we used a western blot to determine if eFn-3A02 or eFn-4B02 were able to block signaling through gp130 (Figure 3A). First, we incubated 50 ng/ml IL-6 with HuH 7.5.1 cells with or without 500 nM engineered 10Fn3 at 37°C for 12 minutes. We tested the effects of eFn-4B02, eFn-3A02, and an unselected control fibronectin that has no effect on IL-6 binding or STAT3 phosphorylation. Cells were lysed on ice immediately after incubation using RIPA buffer (TBS with 1% NP-40 and 0.5% sodium deoxycholate), centrifuged at 20,000×g for ten minutes, and combined with SDS loading buffer. Western blots were probed with mouse anti-human-phospho(Y705)-STAT3 (Cell Signaling Technology) and imaged with film after exposure with ECL. Blots were stripped and re-probed with polyclonal rabbit anti-STAT3 for total STAT3 detection.

While the cysteine-containing eFn-3A02 did not inhibit IL-6 signaling, eFn-4B02 demonstrated significant inhibition at the concentration tested. We next performed quantitative western analysis with a concentration series between 10 nM and 10 μM (Figure 3B). Here, eFn-4B02 and IL-6 (10 ng/ml) were pre-incubated before application to HuH 7.5.1 cells. Western blots were simultaneously probed with mouse monoclonal anti-phospho(Y705)-STAT3 and rabbit monoclonal anti-STAT3 (total) followed by probing with infrared dye-labeled secondary antibodies (LI-COR Biosciences, Lincoln, NE). Blots were imaged

using an Odyssey scanner (LI-COR Biosciences) and band intensities were determined using ImageJ. This experiment was performed entirely in triplicate and was used to generate an IC_{50} by four-parameter non-linear regression (Prism) (Figure 3C).

[1] C. A. Olson, H. I. Liao, R. Sun, R. W. Roberts, *ACS Chem. Biol.* **2008**, *3*, 480.
[2] D. L. Minor, Jr., P. S. Kim, *Nature* **1994**, *367*, 660.
[3] C. K. Smith, J. M. Withka, L. Regan, *Biochemistry* **1994**, *33*, 5510.
[4] G. S. Waldo, B. M. Standish, J. Berendzen, T. C. Terwilliger, *Nat. Biotechnol.* **1999**, *17*, 691.
[5] C. A. Olson, R. W. Roberts, *Protein Sci.* **2007**, *16*, 476.
[6] H. I. Liao, C. A. Olson, S. Hwang, H. Deng, E. Wong, R. S. Baric, R. W. Roberts, R. Sun, *J. Biol. Chem.* **2009**, *284*, 17512.
[7] S. W. Millward, S. Fiacco, R. J. Austin, R. W. Roberts, *ACS Chem. Biol.* **2007**, *2*, 625.
[8] F. L. Rock, X. Li, P. Chong, N. Ida, M. Klein, *Biochemistry* **1994**, *33*, 5146.
[9] R. Liu, J. E. Barrick, J. W. Szostak, R. W. Roberts, *Methods Enzymol.* **2000**, *318*, 268.
[10] F. N. Ishikawa, H. K. Chang, M. Curreli, H. I. Liao, C. A. Olson, P. C. Chen, R. Zhang, R. W. Roberts, R. Sun, R. J. Cote, M. E. Thompson, C. Zhou, *ACS Nano* **2009**, *3*, 1219.